

Comparison of Very Smooth Cell-Model Trajectories Using Four Symplectic and Two Runge-Kutta Integrators

Wm. G. Hoover and Carol G. Hoover

Ruby Valley Research Institute

Highway Contract 60, Box 601, Ruby Valley 89833, NV USA

(Dated: December 3, 2024)

Abstract

Symplectic methods, which are precisely compatible with Liouville’s phase-volume-conservation theorem, are often recommended for computational simulations of Hamiltonian mechanics. Lack of energy drift is an advantage of symplectic methods. But *all* numerical methods are susceptible to chaos, Lyapunov instability, which severely limits the maximum time for which solutions can be “accurate”. The “advantages” of higher-order methods are lost for typical chaotic Hamiltonians. We illustrate these difficulties for a useful reproducible test case, the two-dimensional one-particle cell model. The motion is chaotic and occurs on a three-dimensional constant energy shell. We benchmark the problem with quadruple-precision trajectories using a fifth-order Runge-Kutta and the fourth-order Candy-Rozmus integrator. We compare these benchmark results for accurate particle trajectories to those from six double-precision algorithms, four symplectic and two Runge-Kutta.

Keywords: Chaos, Lyapunov Instability Classical Mechanics, Computational Methods

I. INTRODUCTION

The ongoing computational revolution in physics relies on accurate solutions of fundamental equations, Newton’s (or Lagrange’s or Hamilton’s) Laws of Motion, in the case of classical mechanics. The determinism of these ordinary differential equations is illusory in many cases, as typically the equations are “Lyapunov unstable”. Such instabilities grow exponentially fast, $\simeq e^{\lambda t}$, where λ is the largest Lyapunov exponent of the solution.

Particle mechanics, our own research interest, provides many examples ranging from one-particle chaos to biomolecule simulations using models with many thousands of atomic degrees of freedom¹. We consider here the simplest particle model for chaos, a one-body “cell model” with the periodic four-body cell boundaries shown in **Figure 1**. The resulting motion, approximated with the simplest possible “leapfrog” integrator, described below, is generally Lyapunov unstable.^{2,3} We simplify the initial conditions by starting the particle trajectory in the field-free cell interior. We benchmark this problem with two quadruple-precision integrators using timesteps chosen to maximize accuracy. We compare the resulting benchmark trajectory to six trajectories from self-starting double-precision algorithms typical of molecular dynamics simulations. Four of these algorithms are “symplectic”, including the simplest and popular Leapfrog Algorithm, and two are Runge-Kutta.

In the following Sections we describe the differential equations governing the motion of the wandering cell-model particle, and then quantify the algorithmic accuracy with which Leapfrog and the five more sophisticated integrators “solve” this same problem. Our conclusions make up the final Summary section.

II. THE CELL MODEL TRAJECTORY IN TWO SPACE DIMENSIONS

Cell models played a role in models of the liquid state long before the development of molecular dynamics.⁴ The geometry treated here is shown at the left in **Figure 1**. A mass point, the “wanderer” particle, moves in a periodic square cell with a motionless fixed particle at each of the four vertices. Using periodic boundary conditions the equations of motion are :

$$\dot{x} = (p_x/m) ; \dot{y} = (p_y/m) ; \dot{p}_x = F_x ; \dot{p}_y = F_y .$$

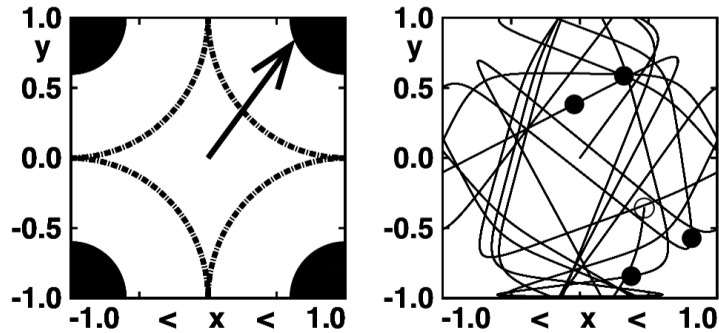


Figure 1: The periodic 2×2 unit cell is shown at the left. The black regions, with potential energy greater than unity are inaccessible to the wanderer particle. Initially the wanderer is at the origin with velocity $(0.6, 0.8)$. Outside the central diamond-shaped region the fixed scatterers at the cell corners exert repulsive forces on the wanderer particle. An accurate trajectory, calculated with a quadruple-precision fifth-order Runge-Kutta integrator, using five million timesteps and $dt = 0.00001$, is shown at the right with filled circles marking the configurations at times 10, 20, 30, and 40. The open circle corresponds to the maximum time $t = 50$.

The force on the wanderer is the gradient of the potential function Φ , a sum over the contributions of the four corner scatterers :

$$\Phi = \sum_1^4 [1 - (r - r_i)^2]^4 \text{ for } |r - r_i| < 1 .$$

After advancing the coordinates one timestep dt it is convenient to localize the motion to the cell centered on the origin. Whenever the wanderer moves “out”, we replace it “in” the basic 2×2 unit cell as follows :

$$x < -1 \rightarrow x = x + 2 ; x > +1 \rightarrow x = x - 2 ;$$

$$y < -1 \rightarrow y = y + 2 ; y > +1 \rightarrow y = y - 2 .$$

We choose initial conditions $\{ x, y, p_x, p_y \} = \{ 0.0, 0.0, 0.6, 0.8 \}$ and show an accurate benchmark solution of the motion equations for a time of 50 at the righthandside of **Figure 1**. At times of 10, 20, 30, 40, and 50 the benchmark values of (x, y) are :

$$10: +0.321356333887505, +0.585921713605895$$

$$20: +0.81481797353866, -0.572042192203162$$

30: -0.040449409487, +0.38290501902

40: +0.3742439, -0.842854

50: +0.4696, -0.3568

Figure 1 shows a unit cell of a periodic two-dimensional lattice in which a single particle moves in the field of scattering particles arranged in a fixed square lattice with nearest-neighbor spacing of 2. The potential energy maximum of unity is twice the energy of the initial condition, shown at the center of the cell. The benchmark solution of the motion equations $\{ \dot{q} = p ; \dot{p} = F(q) \}$ is shown at the right. This same accurate trajectory was obtained with both the Candy-Rozmus fourth-order and a Runge-Kutta fifth-order integrator using 50 million and 500 million timesteps, respectively. The two trajectories agree throughout within visual accuracy. At a time of 50 (x, y, p_x, p_y) are :

$$(x, y, p_x, p_y) = (+0.46961, -0.35683, +0.11945, +0.98408) \text{ [CR4] ;}$$

$$(x, y, p_x, p_y) = (+0.46962, -0.35682, +0.11948, +0.98408) \text{ [RK5] .}$$

III. SIX TYPICAL INTEGRATORS AND THEIR TRAJECTORIES

We consider six solution algorithms for the particle trajectory, [1] Leapfrog (symplectic), [2] Fourth-Order Candy-Rozmus Symplectic, [3] Monte Carlo Symplectic, [4] Sixth-Order Symplectic, [5] Fourth-Order Runge-Kutta, and [6] Fifth-Order Runge-Kutta. For each of these we use a fixed timestep typical of “accurate” molecular dynamics simulations $dt = 0.001$. Solutions for the six integrators appear in **Figures 2-7** . The particle mass is unity and the energy $\Phi + K$ is one half.

A. Second-Order Time-Reversible Leapfrog Algorithm

“Symplectic” integrators⁵⁻⁹ automatically obey Liouville’s Theorem by advancing the solution of Hamiltonian problems in time according to a series of phase-volume-conserving shears. Symplectic algorithms alternate steps advancing the coordinates and momenta in time. The simplest example is equivalent to the Störmer-Verlet “leapfrog algorithm” :⁸⁻¹⁰

$$\{ \mathbf{q} = \mathbf{q} + (\mathbf{p} * dt/2) ; \mathbf{p} = \mathbf{p} + (\mathbf{F}/m) * dt ; \mathbf{q} = \mathbf{q} + (\mathbf{p} * dt/2) \} \longleftrightarrow$$

$$\{ q_{n+1} - 2q_n + q_{n-1} \equiv (F/m)_n \} .$$

This algorithm is said to be “second order”¹⁰, with a fixed-time coordinate error of order tdt^2 for $t \ll 2\pi/dt^2$ when applied to the simple harmonic oscillator. It is time reversible in that changing $+dt \rightarrow -dt$ gives the same trajectory points either forward or backward in time.

How does the simulation begin? Starting out at the origin, with the wanderer speed equal to unity and a fixed timestep $dt = 0.001$, the first 420 steps leave the momenta unchanged and r^2 becomes 1.0004. During the 421st step the upper right scatterer is contacted and begins to repel the wandering particle with a force :

$$F_x = 8(x - 1)(1 - r^2)^3 ; F_y = 8(y - 1)(1 - r^2)^3 ; r = (1 - x, 1 - y) ,$$

where x and y are the wanderer coordinates.

After an elapsed time t we reverse the sign of the time so as to integrate *backward* to see how closely the wanderer returns to its initial location. So long as $t < 47$ we find that the trajectory reverses to within a distance 0.01 of the origin. We will see that this retracing of steps does not guarantee a match with the accurate trajectory shown at the right in **Figure 1**. Both the trajectory reversal and the conservation of energy are poor diagnostics for trajectory *accuracy*, where accuracy means reproducing correct values of the coordinates $x(t), y(t)$.

B. Fourth-Order Time-Reversible Symplectic Integrator

Higher-order algorithms, with fixed-time integration errors of order $dt^3, dt^4, dt^5 \dots$ can be developed from Taylor’s series about t giving small increments in the coordinates and momenta as three-, four-, five- \dots term series in dt . Candy and Rozmus’ fourth-order integrator (with an error of order dt^4 at a fixed not-too-large, time) is a simple example, cited in the very useful summary paper by Gray, Noid, and Sumpter⁷ :

$$q = q + 0.6756036p * dt ; p = p + 1.3512072(F/m) * dt ;$$

$$q = q - 0.1756036p * dt ; p = p - 1.7024144(F/m) * dt ; q = q - 0.1756036p * dt ;$$

$$p = p + 1.3512072(F/m) * dt ; q = q + 0.6756036p * dt .$$

Reference 7 gives the analytic forms of all of the coefficients. Notice that the coefficients incrementing the coordinates sum to unity as do also those incrementing the momenta. Each timestep requires three separate evaluations of the forces.

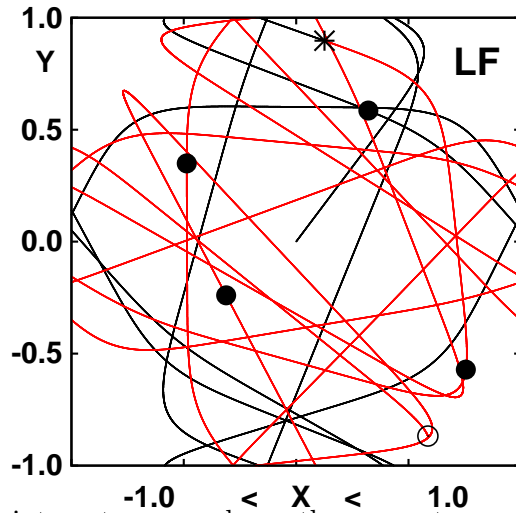


Figure 2: The Leapfrog integrator reproduces the accurate x and y coordinates within 0.01 for an integration time of 18. The energy at that point (where the trajectory color changes, indicated by a star) is in error in the seventh decimal place. Here and elsewhere the cited double-precision times are truncated to integers because different implementations, such as varying the order of the operations, could change these numbers.

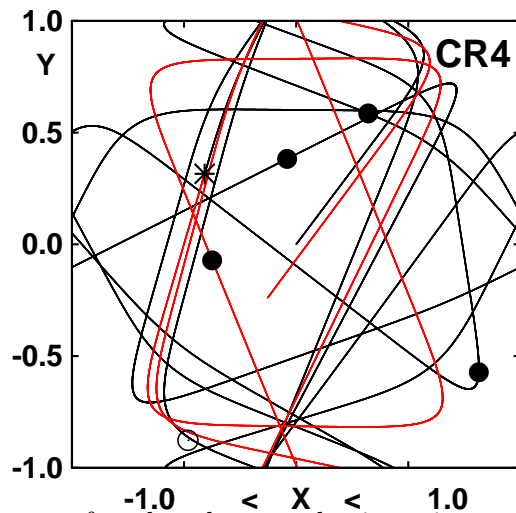


Figure 3: The Candy-Rozmus fourth-order symplectic trajectory exhibits a color change at a time of 34, the maximum for which the coordinate errors are less than 0.01 . The energy error at that time is in the twelfth decimal place. The maximum time at which a reversed trajectory returns to the origin within 0.01 is $t = 42$.

C. Monte-Carlo Time-Reversible Symplectic Integrator

Although it is usual to provide coefficients in integration algorithms to many significant figures, in most cases an approximate rendition is sufficient. It is quite possible to develop algorithms with a Monte Carlo method, adjusting the coefficients to minimize the error for the simple harmonic oscillator problem. An integrator requiring five force evaluations per timestep was developed by Monte Carlo sampling⁶ adjusting the coefficients subject to the constraints of time reversibility and normalization so that the Monte Carlo optimization occurs in a four-dimensional space. The resulting integrator was successful in modelling many-body dynamics but is here applied to the cell-model problem of **Figure 1** :

$$q = q + 0.005904p * dt ; p = p + 0.171669(F/m) * dt ;$$

$$q = q + 0.515669p * dt ; p = p - 0.516595(F/m) * dt ;$$

$$q = q - 0.021573p * dt ; p = p + 1.689852(F/m) * dt ; q = q - 0.021573p * dt ;$$

$$p = p - 0.516595(F/m) * dt ; q = q + 0.515669p * dt ;$$

$$p = p + 0.171669(F/m) * dt ; q = q + 0.005904p * dt .$$

The cell model trajectory using this Monte Carlo integrator is illustrated in **Figure 4**.

D. Yoshida's Sixth-Order Time-Reversible Integrator

Yoshida developed and applied a general technique for finding higher-order symplectic integrators.¹¹ His sixth-order time-reversible integrator advances the coordinates ($\Delta q \propto pdt$) eight times per timestep, using the symmetric (so as to guarantee time-reversibility) set of eight coefficients which sum to unity :

$$+0.39225680523878, +0.51004341191846, -0.47105338540976, +0.06875316825252,$$

$$+0.06875316825252, -0.47105338540976, +0.51004341191846, +0.39225680523878.$$

Between the successive coordinate updates there is a force calculation and an update of the momenta ($\Delta p \propto Fdt$), using seven coefficients, which likewise sum to unity :

$$+0.78451361047756, +0.23557321335936, -1.1776799841789, +1.3151863206839,$$

$$-1.1776799841789, +0.23557321335936, +0.78451361047756.$$

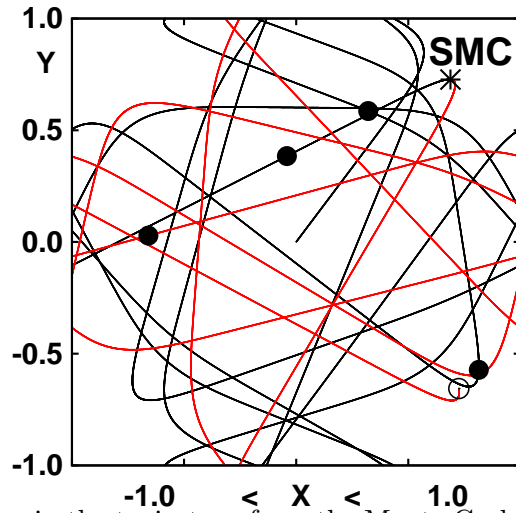


Figure 4: The color change in the trajectory from the Monte Carlo symplectic integrator occurs at a time of 31, after which the coordinate errors exceed 0.01. The energy error there is in the thirteenth digit. For this integrator a trajectory reversed at a time of 43 will return to the origin with coordinates recurring within 0.01.

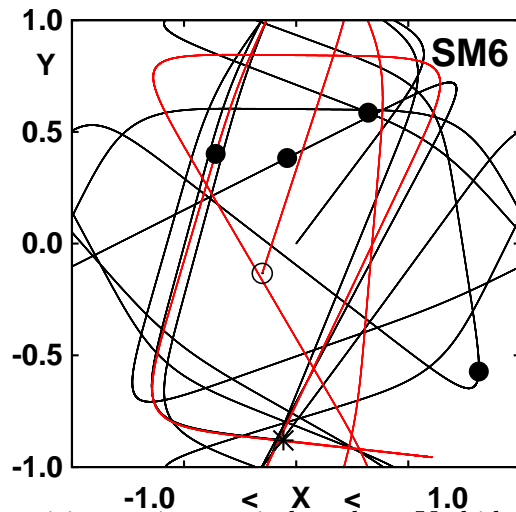


Figure 5: This double-precision trajectory is based on Yoshida's time-reversible sixth-order integrator with a timestep $dt = 0.001$. There is a color change at $t = 36$, indicating the degradation of trajectory accuracy to ± 0.01 despite the negligible energy error in the fourteenth decimal place. Trajectory reversal at a time of 42 returns to the origin within coordinate errors of 0.01.

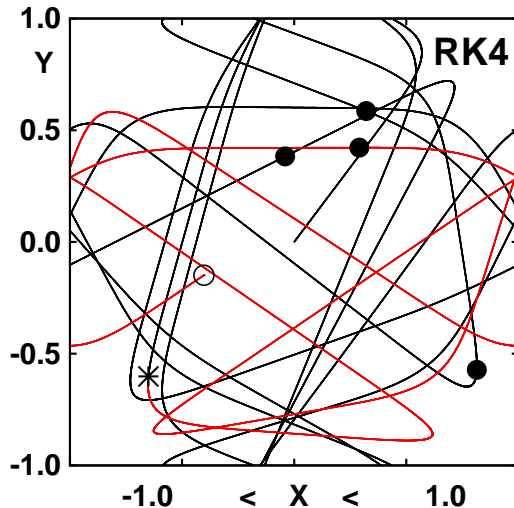


Figure 6: The fourth-order Runge-Kutta trajectory using double precision and a timestep $dt = 0.001$ provides coordinates accurate within 0.01 through a time of 35, indicated by the color change at the star. The energy error at that point, 10^{-13} , is negligible. Changing the sign of the timestep at $t = 42$, $+dt \rightarrow -dt$, returns the trajectory to the origin within a precision of 0.01.

E. Fourth-Order and Fifth-Order Runge-Kutta Integrators

Runge-Kutta integrators (*circa* 1900, as described in Wikipedia) advance both coordinates and momenta *simultaneously* in a series of stages within each timestep dt . As in the symplectic case the variables at time $t + dt$ are expressed as series in dt , putting conditions on the summed-up coefficients for each power of dt to be treated correctly by the algorithm.

The main advantage of Runge-Kutta methods is that they can be applied to arbitrary sets of ordinary differential equations, not just those from Hamiltonian mechanics. The fourth-order “classic” Runge-Kutta method has been a standard workhorse model for solving sets of coupled ordinary differential equations for 100 years. Applied to the harmonic oscillator the fourth-order algorithm suffers a loss in energy proportional to the fifth power of the timestep. The fifth-order Runge-Kutta integrator behaves in the opposite manner with the energy increasing rather than decreasing.

Hybrid “adaptive” models, incorporating both fourth- and fifth-order algorithms, provide a simple means for the automatic control of integration errors. The harmonic oscillator is an excellent test case of integrator accuracy where Lyapunov instability is absent.¹⁰

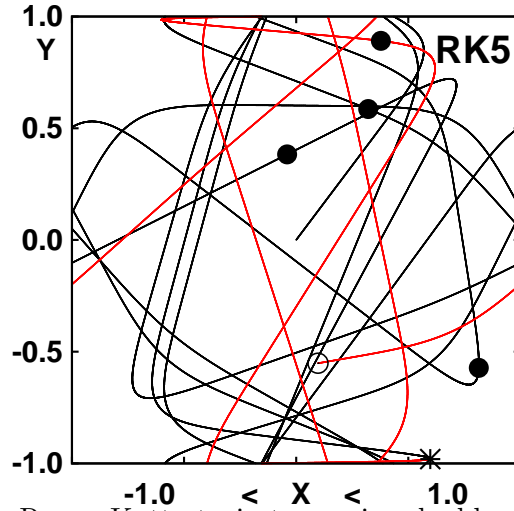


Figure 7: The fifth-order Runge-Kutta trajectory using double precision and a timestep $dt = 0.001$ provides coordinates accurate within 0.01 through a time of 37, indicated by the color change at the star. The energy error at that point is 10^{-14} . For times less than 42 a simple reversing the trajectory by setting $+dt \rightarrow -dt$ returns the trajectory to the origin with precision 0.01. This integrator is the best of the double-precision integrators tested here. Any one of the five higher-order integrators is accurate for about twice the time of the second-order Leapfrog integrator.

Figure 6 illustrates the same cell-model orbit for the classic fourth-order Runge-Kutta integrator. **Figure 7** shows a fifth-order Runge-Kutta integrator :

$$yp1 = yp[y]$$

$$yp2 = yp[y + (dt/2) * yp1]$$

$$yp3 = yp[y + (dt/16) * (3yp1 + yp2)]$$

$$yp4 = yp[y + (dt/2) * yp3]$$

$$yp5 = yp[y + (dt/16) * (-3yp2 + 6yp3 + 9yp4)]$$

$$yp6 = yp[y + (dt/7) * (yp1 + 4yp2 + 6yp3 - 12yp4 + 8yp5)]$$

$$y = y + (dt/90) * (7yp1 + 32yp3 + 12yp4 + 32yp5 + 7yp6)$$

Here $yp[\dots]$ represents the righthandside of the vector differential equation $\dot{y} = y'$ where the six force evaluations in each timestep are indicated by $\{ yp1, yp2, \dots, yp6 \}$.

Both Runge-Kutta integrators return to the origin with errors no more than 0.01 with reversal at time 42. Forward in time their trajectories are accurate through times of 35 and 37, the last being the best of the double-precision integrators. The energy errors for the two Runge-Kutta integrators are in the thirteenth and fourteenth decimal places.

IV. LYAPUNOV INSTABILITY IN THE CELL MODEL

The exponential Lyapunov instability of dynamical systems is easily measured by following the motion of a “reference” trajectory in the usual way, for instance with any one of the six algorithms discussed here. An additional “satellite” trajectory, separated from the reference by a small length δ_0 , is also followed using the same algorithm. At the end of each timestep the separation is rescaled, maintaining the length of the offset between the trajectories constant, but allowing the direction to vary :

$$\delta(t + dt) \equiv [r_s(t + dt) - r_r(t + dt)] ;$$

$$r_s \longrightarrow r_r(t + dt) + \delta(t + dt) [\delta_0 / | \delta(t + dt) |] .$$

The largest Lyapunov exponent is simply the average value of the growth rates measured at the ends of every timestep prior to rescaling :

$$\lambda_1 = \langle (1/dt) \ln [| \delta(t + dt) | / \delta_0] \rangle .$$

Previous studies of this cell model,³ with the same initial condition, have shown that the largest Lyapunov exponent is about 0.7. This means that an error of the order 10^{-16} at the initiation of a run of length 50 will increase by a factor of

$$e^{\lambda t} = e^{0.7 \times 50} = e^{35} \simeq 10^{15} .$$

This exponential growth rate explains why it is that *all* of the double-precision integrators fail, from the standpoint of reproducing a reversible trajectory, at about the same time, at about *half* the time where quadruple-precision trajectories fail. It is because these trajectories are just approximations that the most sophisticated biomolecule simulations are based on the rudimentary leapfrog algorithm rather than more sophisticated algorithms.

Of course, even the slightest difference in the error prior to amplification will yield a different history. Even such a small cause as summing the particle interactions in a

different order leads to qualitatively different histories once the Lyapunov instability rises to the level of visibility, an increase of 16 digits for routine double-precision simulations. The phase-shift errors in all of the algorithms discussed here can be measured by choosing the initial velocity $(\sqrt{1/2}, \sqrt{1/2})$ for which the roundoff errors in the x and y directions are identical.

If high accuracy is required, as in astronomical simulations, multiple precision can be employed, as demonstrated by Lorenz Attractor simulations using a precision of thousands of decimal digits. But, as Joseph Ford was fond of pointing out, Lyapunov instability is incompatible with high accuracy. Doubling the number of significant figures in the integration algorithm only doubles the time for which the simulation is accurate.

Recently Hanno Rein and David Siegel¹² developed and implemented a relatively complicated fifteenth-order integrator for gravitational problems with the provocative title “A Fast, Adaptive, High-Order Integrator for Gravitational Dynamics, Accurate to Machine Precision Over a Billion Orbits”. Evidently this integrator is not at all intended for long-time applications to chaotic problems, where errors grow exponentially with time. Conversations with Ben Leimkuhler and Mark Tuckerman, both of whom summarily dismiss the use of Runge-Kutta techniques, due to their monotonic energy drift, plus the appearance of Rein and Siegel’s high-order long-time work led to the present article.

V. RECENT DEVELOPMENTS AND SUMMARY

To summarize, for simple chaotic simulations (such as classical fluids) symplectic integrators attain accuracies similar to those obtained with Runge-Kutta integration and are primarily limited by Lyapunov instability. Although energy conservation and trajectory reversibility characterize symplectic integrators, those properties do not ensure trajectory accuracy. The reversibility of the double-precision leapfrog integrator, to a time of 47 and back, exceeds that of all the more accurate double-precision integrators.

For us it was illuminating to find that the humble Leapfrog integrator, presumably nearing its 330th anniversary⁸, is nearly as useful as are its more complex relatives, and is certainly far more economical. For higher accuracy there is little distinction between the symplectic and the Runge-Kutta integrators for chaotic problems, because both types lose accuracy at the very same rate, determined by the maximum Lyapunov exponent.

It is significant that all of the integrators used here conserve energy almost perfectly

for the benchmark problem. They also reverse back to the initial conditions *even when their trajectories are inaccurate*. One takeaway message from these simulations is the one to which Joseph Ford devoted much thought and many thought-provoking words, among them these taken from Reference 14 :

“Newtonian determinism assures us that chaotic orbits exist and are unique, but they are nevertheless so complex that they are humanly indistinguishable from realisations of truly random processes.”

Liao has confronted the Lyapunov instability problem headon for the Lorenz Attractor.¹⁵ By using 3500-term series expansions coupled with 4180-digit arithmetic he followed the evolution of the Lorenz Model to a time of 10,000. Like the continuing discovery of the digits of π this activity will last as long as mankind.

Lyapunov instability often shows up in peculiar places. Simply changing the order of operations in adding up forces or in computing the weights of contributions to differential equations’ righthandsides can provide the seeds from which macroscopic change develops. We learned this lesson in simulating the collisions of mirror-image manybody drops and crystals. To retain accurate mirror symmetry it was necessary to symmetrize the force calculations at every timestep.¹⁶

VI. ACKNOWLEDGMENTS

We thank Ben Leimkuhler, Hanno Rein, and Mark Tuckerman for their useful and stimulating comments and Clint Sprott for his constant encouragement. We are grateful to the GNU Fortran project for furnishing their no-cost quadruple-precision compiler. To find it GOOGLE “GNU Fortran project”.

¹ M. Karplus, “ ‘Spinach on the Ceiling’ : a Theoretical Chemist’s Return to Biology”, Annual Review of Biophysics and Biomolecular Structure **35**, 1-47 (2006).

² H. A. Posch, W. G. Hoover, and F. J. Vesely, “Canonical Dynamics of the Nosé Oscillator: Stability, Order, and Chaos”, Physical Review A **33**, 4253-4265 (1986).

³ W. G. Hoover and C. G. Hoover, *Simulation and Control of Chaotic Nonequilibrium Systems* (World Scientific Publishers, Singapore, 2015).

- ⁴ J. A. Barker and D. Henderson, “What is ‘Liquid’ ? Understanding the States of Matter”, *Reviews of Modern Physics* **48**, 587-671 (1976).
- ⁵ B. Leimkuhler and S. Reich, *Simulating Hamiltonian Dynamics* (Cambridge University Press, United Kingdom, 2004).
- ⁶ W. G. Hoover, O. Kum, and N. E. Owens [now Nancy Fulda], “Accurate Symplectic Integrators *via* Random Sampling”, the *Journal of Chemical Physics* **103**, 1530-1532 (1995).
- ⁷ S. K. Gray, D. W. Noid, and B. G. Sumpter, “Symplectic Integrators for Large Scale Molecular Dynamics Simulations: A Comparison of Several Explicit Methods”, the *Journal of Chemical Physics* **101**, 4062-4072 (1994).
- ⁸ E. Hairer, C. Lubich, and G. Wanner, “Geometric Numerical Integration Illustrated by the Störmer-Verlet Method”, *Acta Numerica* **12**, 399-450 (2003).
- ⁹ D. Levesque and L. Verlet, “Molecular Dynamics and Time Reversibility”, *Journal of Statistical Physics* **72**, 519-537 (1993).
- ¹⁰ G. D. Venneri and W. G. Hoover, “Simple Exact Test for Well-Known Molecular Dynamics Algorithms”, *Journal of Computational Physics* **73**, 468-475 (1987).
- ¹¹ H. Yoshida, “Construction of Higher Order Symplectic Integrators”, *Physics Letters A* **150**, 262-268 (1990).
- ¹² H. Rein and D. S. Spiegel, “IAS15: A Fast, Adaptive, High-Order Integrator for Gravitational Dynamics, Accurate to Machine Precision Over a Billion Orbits”, arXiv 1409.4779, also available in the *Monthly Notices of the Royal Astronomical Society*.
- ¹³ W. G. Hoover, J. C. Sprott, and P. K. Patra, “Ergodic Time-Reversible Chaos for Gibbs’ Canonical Oscillator”, (submitted to *Physical Review E*, 2015) = arXiv 1503.06729.
- ¹⁴ J. Ford, “What is Chaos, that We Should be Mindful of It ?”, in *The New Physics*, edited by Paul Davies (Cambridge University Press, 1989).
- ¹⁵ S. Liao, “A Comment on the Arguments about the Reliability and Convergence of Chaotic Simulations”, *International Journal of Bifurcation and Chaos*, **24**, 91450119 (2014) = arXiv 1401.0256.
- ¹⁶ W. G. Hoover and C. G. Hoover, “What is Liquid? Lyapunov Instability Reveals Symmetry-Breaking Irreversibility Hidden within Hamilton’s Many-Body Equations of Motion”, *Condensed Matter Physics* **18**, 13003-1-13 (2015) = arXiv 1405.2485.